# Sixteen-year phytoplankton biomass trends in the northwestern Pacific Ocean observed by the SeaWiFS and MODIS ocean color sensors

**Eko Siswanto · Makio C. Honda · Kazuhiko Matsumoto · Yoshikazu Sasai · Tetsuichi Fujiki · Kosei Sasaoka · Toshiro Saino**

E. Siswanto (⌧) ·Y. Sasai

Japan Agency for Marine-Earth Science and Technology, 3173-25 Showa-machi, Kanazawa-ku, Yokohama, Kanagawa, 236-0001, Japan

e-mail: ekosiswanto@jamstec.go.jp, Tel: +81 45 778 5268, Fax: +81 45 778 5706

M. C. Honda · K. Matsumoto · T. Fujiki · K. Sasaoka · T. Saino

Japan Agency for Marine-Earth Science and Technology, 2-15 Natsushima-cho Yokosuka, Kanagawa, 237-0061, Japan

**Abstract** Using multisensor/platform biophysical data collected from 1997 to 2013, we investigated trends of the concentrations of phytoplankton biomass (Chl) in the northwestern Pacific Ocean (NWPO) and the probable responsible factors. The trend of rising sea surface temperature (SST) was the main factor maintaining phytoplankton positive net growth and resulted in a trend of increasing Chl at high latitudes in all seasons. At latitudes of 36–48°N, east of 160°E, the trend of rising SST was accompanied by a trend of declining Chl, markedly in spring and fall, which could be ascribed to strengthened stratification. The trends of environmental variables in the Oyashio area have modified conditions in a way detrimental to phytoplankton growth, the result being a trend of declining Chl from spring to fall. Chl south of roughly 36°N exhibited different trends in different seasons because of the different trends of vertical stratification.

Whereas the observed 16-year Chl trends were not primarily influenced by interannual climate variability, to some degree they were likely modified by decadal variability associated with a weakened Aleutian Low pressure. This work prompts further comprehensive studies to investigate the probable ecological consequences of the observed Chl trend for high-trophic-level marine organisms in the NWPO.

**Keywords** Remote sensing · Ocean color · Chlorophyll-*a* · Phytoplankton growth · Light/nutrient limitation · Climate change

## 1 Introduction

The northwestern Pacific Ocean (NWPO) consists of a cyclonic subarctic and an anti-cyclonic subtropical gyre. To the west, the subarctic and subtropical gyres are bordered by the Oyashio and the Kuroshio currents, respectively, whereas meridionally, the two gyres are separated by the Kuroshio-Oyashio confluence area (Fig. 1) (Hanawa and Mitsudera 1986; Yasuda 2003). To enable comparative, long-term, biogeochemical studies of the subarctic and subtropical gyres, two biogeochemical time-series stations, K2 (47ºN, 160ºE, subarctic area) and S1 (30ºN, 145ºE, subtropical area), have been established (see Honda et al. this volume).

Stations K2 and S1 exhibit distinct biogeochemical characteristics: at station K2 (S1) nutrient concentrations are high (low), sea surface temperature (SST, ºC) is low (high), the critical depth is shallow (deep), and the winter phytoplankton chlorophyll-*a* concentration (Chl, mg $m^{-3}$) is low (high) (see Siswanto et al. 2015). The distinct geophysical differences between stations K2 and S1 lead to a limitation of phytoplankton growth by light/temperature and nutrients at stations K2 and S1, respectively (e.g., Matsumoto et al. 2014; Siswanto et al. 2015). On the basis of multiplatform-derived biogeochemical data, Siswanto et al. (2015) have shown that not only do light/temperature and nutrient limitation occur at stations K2 and S1, respectively, but also that the limiting factors change meridionally during different seasons as a result of seasonal changes in geophysical variables.

Meridional differences in the variability of phytoplankton Chl emerge not only at seasonal time scales but also at interannual and decadal time scales in response to large-scale climate variability (Goes et al. 2003; Aita et al. 2007; Chiba et al. 2008; Siswanto et al. this volume). By pixel-based spatiotemporal analysis of satellite data, Siswanto et al. (this volume) showed that there exists a meridional difference in the response of Chl to climatic anomalies; i.e., Chl tends to decrease (increase) over the area north (south) of 42$^{o}$N during the positive phase of the Pacific Decadal Oscillation (PDO), even though the forcing factors (e.g., vertical mixing) are the same in the two areas. Such meridional differences are consistent with the meridional difference in phytoplankton limiting factors (e.g., Siswanto et al. 2015).

Considering that NWPO phytoplankton respond differently to the same forcing factor(s) at different latitudes, it is thus likely that whether any geophysical variables (e.g., temperature, vertical mixing, stratification, light) that undergo long-term trends, perhaps because of global warming, lead Chl to increase or decrease depends on latitude. Behrenfeld et al. (2006) and Doney (2006), for instance, have postulated that phytoplankton at high latitudes will indirectly benefit from warming of the ocean, because a warmer ocean weakens vertical mixing and allows phytoplankton to spend more time within the euphotic zone, the result being an increase of Chl. Toseland et al. (2013) also suggest that phytoplankton at high latitudes directly benefit from a warming ocean because rising temperatures promote phytoplankton growth. In contrast, a warmer ocean will be detrimental to phytoplankton (decrease Chl) in low latitudes because of strengthening of stratification, which will reduce vertical nutrient fluxes from deep layers (e.g., Gregg et al. 2005; Polovina et al. 2008; Boyce et al. 2010).

In fact, on a global scale and in terms of annual means, Chl exhibits meridionally different trends, as mentioned by Vantrepotte and Mélin (2009), but the trends are not always consistent with the aforesaid hypotheses, because the Chl in high (low) latitudes does not always increase (decrease) in response to warming (see Fig. 6b in their paper). Their analysis, based on 10-year satellite Chl data, shows that the trend of Chl in the NWPO is less obvious than the analogous trend in the northeastern Pacific Ocean. This difference was possibly caused by cancellation between positive and negative trends in different seasons.

We thus used a longer dataset (16 years, from September 1997 to June 2013) of Chl derived from ocean color sensors to update Chl trends in the NWPO during the most recent decades. We were interested in determining Chl trends in different seasons. Within the same time span, we also used satellite-based and/or reanalyzed geophysical variables that might have caused Chl trends to differ meridionally and seasonally. Understanding Chl trends and the possible underlying factors at seasonal time scales is important; they may bring ecological consequences for the biomass of high-trophic-level marine organisms by shifting the timing of phytoplankton and zooplankton phenology, varying the food resources for juvenile fish in their feeding ground, and shifting the locations of fishing grounds.

## 2 Methodology

### 2.1 Multiplatform data acquisition

We used 16-year (September 1997 to June 2013) monthly composite Chl and photosynthetically available radiation (PAR, Einstein $m^{-2}$ $d^{-1}$) data with a 9-km spatial resolution retrieved by the Sea-viewing Wide Field-of-view Sensor (SeaWiFS) and the Moderate Resolution Imaging Spectroradiometer-Aqua (MODIS). We acquired the SeaWiFS and MODIS data from http://oceancolor.gsfc.nasa.gov. We also used concurrent monthly SSTs retrieved by the Advanced Very High Resolution Radiometer (AVHRR, http://podaac.jpl.nasa.gov/AVHRR-Pathfinder) with 4-km spatial resolution and the MODIS (http://oceancolor.gsfc.nasa.gov) with a 9-km spatial resolution. The variables SST and PAR were analyzed because temperature and light are important phytoplankton-limiting factors, especially in high latitudes of the NWPO (e.g., Siswanto et al. 2015).

To generate recent 16-year wind speed (WS, m $s^{-1}$) data, an important variable driving vertical mixing, we used the Cross-Calibrated Multiplatform (CCMP)- and WindSat-derived WS, both of which we acquired from http://apdrc.soest.hawaii.edu. We also investigated the mixed layer depth (MLD, m), a key variable controlling the degree of light and/or nutrient availability. To generate a MLD dataset within the same time span, we used MLDs from different platforms. One MLD dataset was acquired from the Global Ocean Data Assimilation System (GODAS, https://climatedataguide.ucar.edu) with 1° spatial resolution, and the other was the Argo float-based MLD dataset acquired from the Japan Agency for Marine-Earth Science and Technology (JAMSTEC, http://www.jamstec.go.jp/ARGO/argo_web/argo/index.html).

### 2.2 Data interpolation and transformation

Although satellite remote sensing provides routine and consistent temporal observations, satellite data, especially those retrieved by optical and infrared sensors, can contain gaps due to cloud cover and rain belts. Gaps in satellite data are problematic for pixel-based analyses of long-term trends and correlations between Chl and environmental variables, because both analyses require spatially and temporally complete datasets. Therefore, prior to spatial and temporal analyses, we applied a Data Interpolating Empirical Orthogonal Function (DINEOF) method to the SeaWiFS, MODIS, AVHRR, and Argo float-derived data to construct spatiotemporally complete SeaWiFS (Chl), MODIS (Chl, SST), AVHRR (SST), and Argo float (MLD) datasets.

The applicability and effectiveness of DINEOF to fill in spatiotemporal gaps in satellite data have been demonstrated in previous studies (e.g., Beckers and Rixen, 2003; Alvera-Azcárate et al. 2005; Li and He 2014; Siswanto et al. 2015). DINEOF is able to fill in gaps in pixels and represent spatial features of satellite images even with 80% cloud coverage both in terms of single images (see Alvera-Azcárate et al. 2005) and temporal means (see Li and He 2014). Our 16-year full dataset had mean cloud coverage of 24% and only three images had cloud coverage of >80%. Mean cloud coverage was relatively high at high latitudes >45°N, but was still <60% (data not shown). We thus expected that DINEOF would also work well with our dataset. DINEOF was not applied to GODAS MLD and CCMP WS because there were no spatiotemporal gaps in those datasets.

To ensure compatibility of the Chl and PAR data retrieved by SeaWiFS and MODIS, a pixel-based linear regression was applied for the period from July 2002 to December 2010, when observations by both sensors were available. Regression coefficients obtained in each pixel were then used to transform all MODIS Chl and PAR so that they were compatible with SeaWiFS Chl and PAR. We finally used SeaWiFS Chl and PAR from September 1997 to December 2007 and transformed MODIS Chl and PAR from January 2008 to June 2013 to derive Chl and PAR trends. Because the uncertainty of the SeaWiFS Chl retrieval in the NWPO has been confirmed to be less than ± 35% (Sasaoka et al. 2002), which is the goal for the uncertainty of the NASA ocean color mission Chl product (O'Reilly et al. 1998), we transformed Chl data from MODIS to SeaWiFS.

With the same data transformation, we derived pixel-by-pixel regression coefficients of AVHRR on MODIS SSTs for the period from July 2002 to December 2009, when the AVHRR and MODIS missions overlapped. We used them to transform MODIS SSTs so that they were compatible with AVHRR SSTs. We then used AVHRR SSTs from September 1997 to December 2009 and transformed MODIS SSTs from January 2010 to June 2013 in the subsequent SST trend analysis. We also transformed GODAS MLDs so that they were compatible with Argo float-based, in situ MLDs. Pixel-by-pixel regression coefficients were derived by using MLD datasets collected from January 2007 to June 2013. For further analysis, we used transformed GODAS MLDs from June 1997 to December 2006 and Argo float-based MLDs from January 2007 to June 2013. A similar data transformation was used to transform Windsat WS so that it was compatible with CCMP WS using regression coefficients derived for the observation period (February 2003 to December 2012) when the two datasets overlapped.

Siswanto et al. (2015) have shown that the aforesaid data transformation is effective for making two datasets compatible. The merged datasets are also consistent with measured data at stations K2 and S1, especially for Chl, for which the uncertainty was less than that (±35%) targeted by the NASA Ocean Color mission.

## 2.3 Data analysis

Prior to trend analysis, seasonal means of all variables were removed by subtracting monthly climatological means from the data time series. The trend analysis was therefore based on variable anomalies. Rather than least-squares regressions, we carried out robust regressions on biophysical variable anomalies against time (monthly basis), because robust regressions are less sensitive (than least-squares regressions) to outliers, the implication being that the observed trends are less influenced by extreme anomalies associated with climatic anomalies on both interannual and decadal time scales. Like Vantrepotte and Mélin (2009), we then used the slope of the robust regressions to approximate the trend from 1997 to 2013. The significance of trend was statistically defined by using Mann-Kendall test with 95% confidence level ($p < 0.05$) (e.g., Kahru et al. 2012).

Although the long-term analysis was based on variable anomalies, hereafter we do not explicitly express the 'anomalies' of the variables. Neither do we use the specific variable name for variable anomaly values. We will use 'Chl' interchangeably to refer to Chl in general terms and specifically when we discuss the results of our analysis. We inspected the trends in different seasons, and following Cohen et al. (2009), we divided the boreal seasons as follows: winter, from January to March; spring, from April to June; summer, from July to September; and fall, from October to December.

## 3 Results and discussion

Phytoplankton Chl is a measure of phytoplankton standing stock, the spatiotemporal variability of which can be an indication of phytoplankton net growth rate, basically determined by the imbalance between phytoplankton growth and loss rates (Irwin and Finkel 2008; Behrenfeld 2010; Marañón et al. 2014). A change in an environmental variable can change environmental conditions in a way that is detrimental and/or favorable for phytoplankton net growth as manifested by Chl changes. For instance, increasing SST stimulates the net growth of phytoplankton at high latitudes (where nutrients are not limiting factor) because it suppresses vertical mixing (thereby shortening the period of time phytoplankton spend in deep, dimly lit waters) and promotes phytoplankton growth (Eppley 1972; Behrenfeld and Falkowski 1997; Behrenfeld et al. 2006; Doney 2006; Toseland et al. 2013). On the other hand, increasing SST is detrimental for phytoplankton in low latitudes where their growth is limited by nutrients, because it strengthens stratification and thereby limits the supply of nutrients from deep layers (Gregg et al. 2005; Polovina et al. 2008; Boyce et al. 2010).

Because phytoplankton limiting factors also change seasonally and meridionally (e.g., Siswanto et al. 2015), long-term changes of environmental conditions would likely affect phytoplankton growth (or precede Chl trends) differently in different seasons and regions. Below, divided into four seasons, we discuss the probable mechanisms underlying the trends of Chl observed in various areas as summarized in Table 1.

## 3.1 Trends of Chl and probable responsible factors in different seasons

### *3.1.1 Winter season*

In high latitudes mainly north of 42°N, Chl tended to increase at a rate of 0.006 mg $m^{-3}$ $yr^{-1}$ and it increased by 0.090 mg $m^{-3}$ within 16 years (Fig. 2a). Increased Chl indicated that over the 16-year period, environment conditions there have changed and become more favorable to positive net growth. Considering the facts that, 1) phytoplankton at high latitudes were limited by light and temperature [inferred from the negative coefficient of correlation (*r*) between Chl and MLD (Fig. 3a), positive *r* between Chl and PAR (Fig. 3b), and positive *r* between Chl and SST (Fig. 3c); see also Fujiki et al. (2014) and Matsumoto et al. (2014)]; and 2) PAR showed no trend (Fig. 2b), the increasing trend of SST might thus produce favorable conditions that would allow phytoplankton net growth to increase, as manifested by an increase of Chl. Moreover, the increasing trend of the MLD (due to increased WS, Figs. 2d, e), rather than being detrimental (by lengthening the low-light period), has likely caused environment conditions to be more favorable for positive net growth through a dilution effect that reduced grazing pressure (e.g., Yoshie et al. 2003; Matsumoto et al. 2014).

However, the most prominent trend of increasing SST at latitudes of 36–42°N (Fig. 2c) was not accompanied by a remarkable Chl trend (Fig. 2a). This finding can be explained by the fact that light was a more important limiting factor than temperature, as evidenced by the lower positive *r* between Chl and SST (Fig. 3c) than between Chl and PAR (Fig. 3b) and the large negative *r* between Chl and MLD (Fig. 3a).

Over the area roughly south of 30°N, a small but significant decreasing trend in Chl was observed (Fig. 2a). It changed at a rate of -0.002 mg $m^{-3}$ $yr^{-1}$ (declined by 0.036 mg $m^{-3}$ in 16 years). The area south of 30°N is a nutrient-limited environment [see the positive *r* for Chl vs MLD (Fig. 3a) and the negative *r* for Chl vs SST (Fig. 3c)] because the MLD south of 30°N is shallower than the critical depth throughout the year (Obata et al. 1996; Siswanto et al. 2015). Therefore, a decreasing trend in MLD south of 30°N (Fig. 2d) might change environment conditions in a way detrimental (by declining nutrient availability) for phytoplankton, the result being a decrease of Chl.

### *3.1.2 Spring season*

Phytoplankton Chl north of 46°N tended to increase (Fig. 2f) at a rate of 0.014 mg $m^{-3}$ $yr^{-1}$ and increased by 0.208 mg $m^{-3}$ over the 16-year time span. Environmental conditions have likely changed in a way more favorable for phytoplankton positive net growth. The increase of growth was likely due to the increasing trend of SST (Fig. 2h).  This hypothesis is supported by the facts that, 1) Chl was positively correlated with PAR and SST (Figs. 3e, f), the suggestion being that phytoplankton growth was controlled by light and temperature; and 2) PAR tended to decline (Fig. 2g).

A trend of decreasing Chl at a rate of 0.008 mg $m^{-3}$ $yr^{-1}$ (decreased by 0.118 mg $m^{-3}$ over the 16 years) at latitudes of 36–46°N, east of 160°E was apparent (Fig. 2f). Although light and temperature were still limiting factors [see the positive *r* between Chl and PAR and Chl and SST (Figs. 3e, f)], the concomitant trend of increasing SST (Fig. 2h) did not cause an increasing trend of net positive growth. Decreased light availability [due to decreased PAR (Fig. 2g)] and decreased nutrient availability (due to strengthened stratification attributed to higher SSTs) were likely responsible for the declining trend in phytoplankton net growth, the result being a decline in Chl. The trend of decreasing MLD in the winter (Fig. 2d) might also have reduced the availability of nutrients that could be consumed by phytoplankton in the spring. Goes et al. (2000, 2003) also mentioned that nutrients entrained by winter vertical mixing is crucial in determining the magnitude of spring Chl.

The most prominent trend of decreasing Chl at a rate of 0.041 mg $m^{-3}$ $yr^{-1}$, however, was observed in the Oyashio area, where Chl declined by 0.622 mg $m^{-3}$ over the 16 years. The negative *r* between Chl and MLD (Fig. 3d) and positive *r* between Chl and PAR (Fig. 3e) in the Oyashio area indicated that phytoplankton growth was more limited by light than by nutrients (e.g., Saito et al. 2002; Liu et al. 2004; Siswanto et al. 2015). Thus, the trends of declining PAR and increasing MLD (due to strengthened WS, Figs. 2i, j) that lengthened the low-light period were detrimental to phytoplankton net growth. This cause-and-effect reflects the fact that the MLD is about the same as the critical depth in the Oyashio area during the spring (Siswanto et al. 2015). The change of environmental conditions in a way detrimental to phytoplankton net growth might also be ascribed to the trend of decreasing SST (due to increased MLD) that reduced phytoplankton growth.

A small but significant trend of increasing Chl at a rate 0.003 mg $m^{-3}$ $yr^{-1}$ (increased by 0.048 mg $m^{-3}$ within 16 years) was observed south of Japan centered at 30ºN (Fig. 2f). The positive *r* between Chl and MLD (Fig. 3d) and negative *r* between Chl and SST (Fig. 3f) indicated that phytoplankton growth in this area was more limited by nutrients than by light. The trend of increasing Chl there was thus likely attributable to a trend of increasing nutrient availability associated with the trend of surface cooling (Fig. 2h) caused by strengthened wind-driven vertical mixing (see strengthened WS and increased MLD in Figs. 2i, j).

### *3.1.3 Summer season*

Summer Chl north of roughly 45°N tended to increase (Fig. 2k) at a rate of 0.015 mg $m^{-3}$ $yr^{-1}$ and increased by 0.217 mg $m^{-3}$ in 16 years. Summer phytoplankton growth at high latitudes was more controlled by temperature and/or light than by nutrients (Figs. 3h, i, see also Kudo et al. 2006; Fujiki et al. 2014; Matsumoto et al. 2014) because winter mixing-entrained nutrients are not fully consumed by phytoplankton, even during the summer. Because PAR tended to decline (Fig. 2l), phytoplankton north of 45°N likely still benefited from the trend of increasing SST (Fig. 2m), and their net growth tended to be positive within the 16-year time span.

In the Oyashio area, Chl tended to decline at rate of 0.018 mg $m^{-3}$ $yr^{-1}$ and declined by 0.248 mg $m^{-3}$ over the study period. The correlations between Chl and MLD were both negative and positive (Fig. 3g), but the correlations between Chl and PAR were consistently positive (Fig. 3h), and the correlations between Chl and SST were consistently negative (Fig. 3i). These relationships indicate that phytoplankton growth was regulated by an interplay between light and nutrient availability. As a resource, light was likely not severely limiting (as it was at high latitudes), and nutrients were not severely limiting (as they were at low latitudes) until an environmental change reduced one of the resources. Thus, the trends of declining nutrient concentrations (due to decreased MLD, Fig. 2n), declining PAR, and perhaps increasing grazing pressure (due to decreased MLD) were among the probable factors driving the trend of declining Chl. The increasing trend of SST was unlikely to cause phytoplankton growth to increase, as temperature was not a limiting factor in the Oyashio area (see Fig. 3i).

The prominent trend of increasing Chl at a rate of 0.004 mg $m^{-3}$ $yr^{-1}$ (increased by 0.053 mg $m^{-3}$ within the 16 years) was also observed over an elongated area from latitude 36ºN northeastward (Fig. 2k), where nutrient limitation is expected to occur due to strong summer stratification [see the positive *r* between Chl and MLD (Fig. 3g) and the negative *r* between Chl and SST (Fig. 3i)]. The factors responsible for the trend of increasing Chl are unclear, because the observed trends of increasing SST and decreasing MLD (due to increased SST and decreased WS, Fig. 2o) were expected to cause Chl to decrease by reducing nutrient availability and increasing grazing pressure.

### *3.1.4 Fall season*

Fall Chl north of 45ºN increased at a rate of 0.012 mg $m^{-3}$ $yr^{-1}$ and increased by 0.176 mg $m^{-3}$ within 16 years (Fig. 2p). Rather than nutrients, light and temperature were the controlling factors for phytoplankton growth (see the positive *r* values between Chl and PAR and between Chl and SST in Figs. 3k, l). Therefore, the accompanying trends of increasing PAR and SST (Figs. 2q, r) modified environmental conditions in a way favorable for phytoplankton positive net growth.

Over the area from the Oyashio area eastward along latitudes of 42–48°N, Chl tended to decline at a rate of 0.009 mg $m^{-3}$ $yr^{-1}$ and it decreased by 0.134 mg $m^{-3}$ within 16 years (Fig. 2p). Although PAR and SST were still important controlling factors (see the positive *r* between Chl and PAR and between Chl and SST, Figs. 3k, l), a prominent trend of increasing SST (Fig. 2r) was unable to cause a trend of increasing positive net growth. Therefore, the trends of decreasing PAR [to reduce light availability, (Fig. 2q)] and decreasing MLD [to increase grazing pressure, (Fig. 2s)] might be responsible for the decreasing net growth over the 16-year time span, as manifested by the declining trend of Chl. The decreased MLD in this latitude band can also be ascribed to both increased SST and decreased WS (Fig. 2t).

A prominent trend of declining Chl at latitudes of 33–42°N and east of 160°E at a rate of 0.005 mg $m^{-3}$ $yr^{-1}$ (decreased by 0.078 mg $m^{-3}$ in 16 years) was likely caused by a tendency of declining nutrient availability attributed to a warming trend of SST. Phytoplankton growth south of 42°N was likely controlled by nutrients [see the negative *r* between Chl and SST (Fig. 3l)] especially south of 36°N [see the positive *r* between Chl and MLD (Fig. 3j)]. Over the western area south of Japan, the trend of decreasing MLD likely reduced nutrient availability and was the cause of the trend of declining Chl there. The warming trend of SST that strengthened stratification in the eastern area south of 30°N was likely responsible for the small but significant trend of declining Chl a rate of about 0.001 mg $m^{-3}$ $yr^{-1}$ (declined by 0.018 mg $m^{-3}$ in 16 years).

## 3.2 Relevance to previous studies and discrepancies

When all seasons are included, annual mean Chl in the subarctic area north of roughly 45°N tended to increase (Fig. 4a). As discussed above, the trend of increasing SST, by driving the trend of increasing phytoplankton positive net growth in all seasons, was the main factor responsible for this Chl increase. Considering only significant increasing trends ($p < 0.05$), annual mean Chl north of 45°N increased by 0.095 mg $m^{-3}$ within the 16-year period of study. Previous studies that included all seasons reported different Chl trends in the NWPO due to different periods of the SeaWiFS records and approaches. For instance, by executing linear regression analysis on all data (including Chl data during El Niño and La Niña periods) McClain et al. (2004) and Gregg et al. (2005) reported a declining trend of Chl within a period of 6 years prior to 2003. On the other hand, Behrenfeld et al. (2006) suggested a trend of increasing Chl in the NWPO from 1999 to 2004, because they excluded Chl data from the 1997 El Niño and 1988 La Niña periods. These results indicate that a short time series of Chl is greatly influenced by El Niño/Southern Oscillation (ENSO) variability, and thus is insufficient to derive long-term trends of Chl.

Using a 10-year (from November 1997 to October 2007) SeaWiFS Chl record that included all seasons, Vantrepotte and Mélin (2009) suggested that, except for the tropical oceans, the overall pattern of Chl trends with and without data from El Niño and La Niña periods are similar, the implication being that the temporally short climate variability of ENSO did not mainly drive the 10-year trend of Chl in the NWPO, which showed a trend of increasing Chl almost over the entire NWPO (see their Fig. 6b). With a robust regression analysis and using the same 10-year Chl data, we found patterns of Chl trends (Fig. 4b) similar to the results of Vantrepotte and Mélin (2009).

Extending satellite Chl record to June 2013 (16-year time span), we found an overall Chl trend (Fig. 4a) different from Vantrepotte and Mélin’s (2009) result or our result with a 10-year data record (Fig. 4b). Spatial variation of the trend in Fig. 4a was the result of using the full Chl dataset (gap-filled, and including El Niño and La Niña periods). The features in Fig. 4a also appeared in Fig. 4c, which was the result of excluding data from strong/moderate El Niño and La Niña periods (Fig. 4c). We also found that the spatial feature of Chl trends derived from the original (with gaps) Chl data (Fig. 4d) resembled that derived from the full (gap-filled) Chl dataset (Fig. 4a). This result indicated that the ENSO variability and the use of interpolated (gap-filled) Chl data had little effect on the observed 16-year Chl trends.

As discussed above, the ENSO variability was not superimposed on Vantrepotte and Mélin's (2009) 10-year and our 16-year Chl trends. Therefore, the discrepancy between Chl trends derived from 10-year and 16-year Chl records is probably associated with longer (decadal) variability. The Aleutian Low pressure (ALP) has tended to weaken, as indicated by the trend of decreasing PDO index (compared to the strengthening trend before October 2007, Fig. 5). Especially since October 2007, the PDO index has been in large negative phases (mean: –0.87, compared to 0.06 before October 2007). A weakening ALP is known to spin down the cyclonic subarctic gyre (to weaken Ekman divergence) and the anti-cyclonic subtropical gyre (to weaken Ekman convergence) (Sugimoto and Hanawa 2009). The weakened Ekman divergence in the subarctic region might be one reason for the trend of increasing SST at high latitudes (Figs. 2c, h, m, r), which in turn led to a more remarkable trend of increasing Chl compared to the trend before October 2007 (Figs. 4b, 5a). On the other hand, although weakened Ekman convergence in the subtropical region is expected to decrease SST (Figs. 2c, h, m, r), Chl was almost constant (Fig. 5b) because Chl in the subtropical region is no longer limited by temperature.

### 3.3 Probable consequences on marine ecosystems

The increase of SSTs at high latitudes during the winter and spring over the 16 years implies a tendency toward strengthened stratification. The spring bloom onset is expected to advance over the 16-year time span, and perhaps in the future, if such a trend of increasing SST continues (Peeters et al. 2007; Chiba et al. 2008). In contrast, a cooler

SST in low latitudes (including the areas east of Japan) would likely delay the onset of the spring bloom. The changes in phytoplankton phenology is further expected to influence zooplankton phenology (e.g., Chiba et al. 2008) and perhaps fisheries resources in this area.

Besides being influenced by changes of phytoplankton phenology, higher trophic level marine organisms are expected to have been influenced by the changes of Chl and SST over the 16-year period. For instance, the Oyashio area, one of the most productive areas in the world, is an important feeding ground for Japanese sardine and Pacific saury (e.g., Sakurai et al. 2007 and reference therein). They feed on calanoid zooplankton that graze on phytoplankton. The trend of decreasing Chl, especially during spring and summer (the feeding period), might affect recruitment of sardine and saury. The fact that the biomass of saury tended to decrease from 2004 to 2010 and that the spawning biomass of sardine tended to decline from the mid-1990s to 2004 (Sakuramoto et al. 2010; Ito et al. 2013 and reference therein) should prompt more comprehensive studies to investigate whether this decline of a fisheries biomass is related to a declining trend of Chl in the Oyashio area. The north-south contrast of SST trends east of Japan (Figs. 2c, h, m, r) is also expected to influence biomass and fishing ground of saury, because saury feeding and spawning migrations are regulated by SST in this region (see Fig. 2 and Fig. 3 in Ito et al. 2013).

It is probably also of interest to investigate whether the standing stock and fishing ground of albacore in the NWPO have also changed because, 1) the main albacore fishing ground during the fall is over almost the entire latitude band of 36–42°N and east of 160°E, an area that showed the most prominent trends of increasing SST and declining Chl, especially in fall (Figs. 2p, r) (see also Fig. 6 in Zainuddin et al. 2008); 2) albacore fishing ground corresponds with the areas with SST range of 18.5–21.5°C and Chl range of 0.2–

0.4 mg m$^{-3}$ (Zainuddin et al. 2008); and 3) these Chl and SST ranges might shift spatially because of the Chl and SST trends, and so might the albacore fishing ground.

## 4 Summary

Phytoplankton Chl at high latitudes in the NWPO has tended to increase, but with different spatial scales in different seasons. Such a trend of increasing Chl reflected a change of environmental conditions that were able to keep phytoplankton growth greater than losses, the result being phytoplankton positive net growth. We conclude that the trend of increasing SST is the main factor maintaining phytoplankton positive net growth at high latitudes north of roughly 45°N. In the mid-latitudes (~36–46°N and east of 160°E), despite a trend of increasing SST, Chl has tended to decline. The trend of increasing SST (to strengthen stratification) likely changed environmental conditions in a way that resulted in a negative net growth, as manifested by the trend of declining Chl. In the Oyashio area, although environmental variables showed different trends in different seasons, the changed environmental conditions were likely detrimental for phytoplankton net growth, the result being a trend of declining Chl from spring to fall. At latitudes south of 36°N, Chl exhibited different trends in different seasons; these differences might be attributable to the trend of nutrient availability associated with MLD trends. The NWPO Chl trends within the 16-year time span were not primarily influenced by the ENSO interannual variability. However, they were likely modified by the PDO, which has been in a very negative phase (weakened ALP) since 2007. This work suggests that through coupled atmosphere-ocean interactions, climate-driven long-term changes of environmental variables drove the trend of phytoplankton biomass; this work should prompt further study to investigate the ecological consequences for high-trophic-level marine organisms in the NWPO.

**Acknowledgements** This work was partially supported by the Asia-Pacific Network for Global Change Research (APN, CAF2015-RR11-NMY-Siswanto). We thank the Ocean Biology Processing Group (Code 614.2) at the Goddard Space Flight Center, Greenbelt, Maryland, USA, for the production and distribution of their ocean color data. We also acknowledge the Remote Sensing Systems and Physical Oceanography-Distributed Active Archive Center (PO.DAAC), Jet Propulsion Laboratory, for processing and distributing SST and microwave-sensor-retrieved satellite data, respectively. We are grateful to three reviewers whose helpful comments, suggestions, and instructions substantially improved the paper.

## References

Aita MN, Yamanaka Y, Kishi MJ (2007) Interdecadal variation of the lower trophic ecosystem in the northern Pacific between 1948 and 2002, in a 3-D implementation of the NEMURO model. Ecol Model 202(1-2): 81–94. doi:10.1016/j.ecolmodel.2006.07.045

Alvera-Azcárate A, Barth A, Beckers JM (2005) Reconstruction of incomplete oceanographic data sets using empirical orthogonal functions: application to the Adriatic Sea surface temperature. Ocean Model 9(4): 325–346. doi:10.1016/j.ocemod.2004.08.001

Beckers JM, Rixen M (2003) EOF calculation and data filling from incomplete oceanographic datasets. J Atmos Ocean Tech 20(12): 1839–1856. doi: http://dx.doi.org/10.1175/1520-0426(2003)020<1839:ECADFF>2.0.CO;2

Behrenfeld MJ, Falkowski PG (1997) Photosynthetic rates derived from satellite-based chlorophyll concentration. Limnol Oceanogr 42(1): 1–20. doi: 10.4319/lo.1997.42.1.0001

Behrenfeld MJ, O'Malley RT, Siegel DA et al (2006) Climate-driven trends in contemporary ocean productivity. Nature 444: 752–755. doi:10.1038/nature05317

Behrenfeld MJ (2010) Abandoning Sverdrup's Critical Depth Hypothesis on phytoplankton blooms. Ecology 91(4): 977–989. doi: 10.1890/09-1207.1

Boyce DG, Lewis MR, Worm B (2010) Global phytoplankton decline over the past century. Nature 466: 591–596. doi:10.1038/nature09268

Chiba S, Aita MN, Tadokoro K et al (2008) From climate regime shifts to lower-trophic level phenology: Synthesis of recent progress in retrospective studies of the western North Pacific. Prog Oceanogr 77(2-3): 112–126. doi:10.1016/j.pocean.2008.03.004

Cohen J, Barlow M, Saito K (2009) Decadal fluctuations in planetary wave forcing modulate global warming in late boreal winter. J Climate 22: 4418–4426. doi: http://dx.doi.org/10.1175/2009JCLI2931.1

Doney SC (2006) Oceanography: Plankton in a warmer world. Nature 444: 695–696. doi:10.1038/444695a

Eppley RW (1972) Temperature and phytoplankton growth in the sea. Fish Bull 70(4): 1063–1085

Fujiki T, Matsumoto K, Mino Y et al (2014) Seasonal cycle of phytoplankton community structure and photophysiological state in the western subarctic gyre of the North Pacific. Limnol Oceanogr 59(3): 887–900. doi: 10.4319/lo.2014.59.3.0887

Goes JI, Saino T, Oaku H et al (2000) Basin scale estimates of sea surface nitrate and new production from remotely sea surface temperature and chlorophyll. Geophys Res Lett 27(9): 1263–1266. doi: 10.1029/1999GL002353

Goes JI, Gomes HR, Limsakul A et al (2003) The influence of large-scale environmental changes on carbon export in the North Pacific Ocean using satellite and shipboard data.

Deep-Sea Res II 51(1-3): 247–279. doi:10.1016/j.dsr2.2003.06.004
Gregg WW, Casey NW, McClain CR (2005) Recent trends in global ocean chlorophyll. Geophys Res Lett 32: L03606. doi:10.1029/2004GL021808
Hanawa K, Mitsudera H (1986) Variation of water system distribution in the Sanriku Coastal Area. J Oceanogr 42(6): 435–446. doi: 10.1007/BF02110194
Honda MC Matsumoto K, Fuijiki T et al (2015) Ecosystem and material cycle changes caused by climate change estimated from time-series observations in the western North Pacific: an overview of the K2S1 project. J Oceanogr (this volume)
Irwin AJ, Finkel ZV (2008) Mining a sea of data: Deduction the environmental controls of ocean chlorophyll. PLoS ONE 3(11): e3836. doi:10.1371/journal.pone.0003836
Ito SI, Okunushi T, Kishi MJ et al (2013) Modelling ecological responses of Pacific saury (*Cololabis saira*) to future climate change and its uncertainty. ICES J Mar Sci 70(5): 980–990. doi:10.1093/icesjms/fst089
Kahru M, Kudela RM, Manzano-Sarabia M et al (2012) Trends in the surface chlorophyll of the California Current: Merging data from multiple ocean color satellite. Deep Sea Res II 77–80: 89–98. doi:10.1016/j.dsr2.2012.04.007
Kudo I, Noiri Y, Nishioka J et al (2006) Phytoplankton community response to Fe and temperature gradients in the NE (SERIES) and NW (SEEDS) subarctic Pacific Ocean. Deep Sea Res II 53(20-22): 2201–2213. doi:10.1016/j.dsr2.2006.05.033
Li Y, He R (2014) Spatial and temporal variability of SST and ocean color in the Gulf of Maine based on cloud-free SST and chlorophyll reconstructions in 2003-2012. Remote Sens Environ (144): 98–108. doi:10.1016/j.rse.2014.01.019

Liu H, Suzuki K, Saito H (2004) Community structure and dynamics of phytoplankton in the western subarctic Pacific Ocean: A synthesis. J Oceanogr 60(1): 119–137. doi:10.1023/B:JOCE.0000038322.79644.36

Marañón E, Cermeño P, Huete-Ortega M et al (2014) Resource supply overrides temperatures as a controlling factor of marine phytoplankton growth. PLoS ONE 9(6): e99312. doi:10.1371/journal.pone.0099312

Matsumoto K, Honda MC, Sasaoka K et al (2014) Seasonal variability of primary production and phytoplankton biomass in the western Pacific subarctic gyre: Control by light availability within mixed layer. J Geophys Res-Oceans 119(9): 6523–6534. doi:10.1002/2014JC009982

McClain CR, Signorini SR, Christian JR (2004) Subtropical gyre variability observed by ocean-color satellites. Deep Sea Res 51(1-3): 281–301. doi:10.1016/j.dsr2.2003.08.002

Obata A, Ishizaka J, Endoh M (1996) Global verification of critical depth theory for phytoplankton bloom with climatological in situ temperature and satellite ocean color data. J Geophys Res-Oceans 101(C9): 20657 – 20667. doi: 10.1029/96JC01734

O'Reilly JE, Maritorena S, Mitchell G et al (1998) Ocean color chlorophyll algorithm for SeaWiFS. J Geophys Res-Oceans 103(C11): 24937–24953. doi: 10.1029/98JC02160

Peeters F, Straile D, Lorke A et al (2007) Earlier onset of the spring phytoplankton bloom in lakes of the temperate zone in a warmer climate. Glob Change Biol 13(9): 1898–1909. doi: 10.1111/j.1365-2486.2007.01412.x

Polovina JJ, Howell EA, Abecassis M (2008) Ocean's least productive waters are expanding. Geophys Res Lett 35(3): L03618. doi: 10.1029/2007GL031745

Saito H, Tsuda A, Kasai H (2002) Nutrient and plankton dynamics in the Oyashio region of the western subarctic Pacific Ocean. Deep Sea Res II 49(24–25): 5463–5486. doi:10.1016/S0967-0645(02)00204-7

Sakurai Y (2007) An overview of the Oyashio ecosystem. Deep Sea Res II 54(23-26): 2526–2542. doi: 10.1016/j.dsr2.2007.02.007

Sakuramoto K, Shimoyama S, Suzuki N (2010) Relationships between environmental conditions and fluctuations in the recruitment of Japanese sardine, Sardinops melanostictus, in the northwestern Pacific. Bull Jpn Soc Fish Oceanogr 74(2): 88–97

Sasaoka K Saitoh SI, Asanuma I et al (2002) Temporal and spatial variability of chlorophyll-a in the western subarctic Pacific determined from satellite and ship observations from 1997 to 1999. Deep Sea Res II 49(24-25): 5557–5576. doi:10.1016/S0967-0645(02)00206-0

Siswanto E, Honda MC, Sasai Y et al (submitted) Meridional and seasonal footprints of the Pacific Decadal Oscillation on phytoplankton biomass in the northwestern Pacific Ocean. J Oceanogr (this volume)

Siswanto E, Matsumoto K, Honda MC et al (2015) Reappraisal of meridional differences of factors controlling phytoplankton biomass and initial increase preceding seasonal bloom in the Northwestern Pacific Ocean. Remote Sens Environ 159: 44–56. doi:10.1016/j.rse.2014.11.028

Sugimoto S, Hanawa K (2009) Decadal and interdecadal variations of the Aleutian Low activity and their relation to upper oceanic variations over the North Pacific. J Meteo Soc Japan II 87(4): 601–614

Toseland A Daines SJ, Clark JR et al (2013) The impact of temperature on marine phytoplankton resource allocation and metabolism. Nat Clim Change 3: 979–984. doi:10.1038/nclimate1989

Vantrepotte V, Mélin F (2009) Temporal variability of 10-year global SeaWiFS time-series of phytoplankton chlorophyll a concentration. ICES J Mar Sci 66(7): 1547–1556. doi: 10.1093/icesjms/fsp107

Yasuda I (2003) Hydrographic structure and variability in the Kuroshio-Oyashio transition area. J Oceanogr 59(4): 389–402. doi: 10.1023/A:1025580313836

Yoshie N, Yamanaka Y, Kishi MJ et al (2003) One dimensional ecosystem model simulation of the effects of vertical dilution by the winter mixing on the spring diatom bloom. J Oceanogr 59(5): 563–571. doi: 10.1023/B:JOCE.0000009586.02554.d3

Zainuddin M, Saitoh K, Saitoh SI (2008) Albacore (*Thunnus alalunga*) fishing ground in relation to oceanographic condition in the western North Pacific Ocean using remotely sensed satellite data. Fish Oceanogr 17(2): 61–73. doi: 10.1111/j.1365-2419.2008.00461.x

## Figure Captions

**Fig. 1** Map of the study region showing the surface currents, including the Kuroshio (K), Kuroshio extension (KE), Oyashio (O), subarctic front (SF), and East Kamchatka (EK). The letters SO indicate the Sea of Okhotsk. Dashed ellipse indicates approximately the Oyashio area.

**Fig. 2** Spatial variations of significant trends during the winter ($p < 0.05$) for (a) Chl, (b) PAR, (c) SST, (d) MLD, and (e) WS derived from winter monthly data within the study period. The areas with insignificant trends are masked out (white areas). Panels (f–j), (k–o), and (p–t) are the same as panels (a–e), except that the analyses were conducted for spring, summer, and fall, respectively.

**Fig. 3** Spatial variations of significant ($p < 0.05$) correlation coefficients ($r$) between Chl and MLD (a), Chl and PAR (b), and Chl and SST (c) during the winter. The areas with insignificant $r$ are masked out (white areas). Panels (d–f), (g–i), and (j–l) are the same as panels (a–c), except that the analyses were conducted for spring, summer, and fall, respectively.

**Fig. 4** Spatial variation of annual mean Chl significant trends ($p < 0.05$) derived by different procedures. (a) Trend was derived by using the full Chl dataset, i.e., gap-filled data within the 16-year period. (b) Same as panel (a), except within the 10-year period from November 1997 to September 2007. (c) Same as panel (a), except that the trend was derived by excluding Chl data during strong/moderate El Niño and La Niña periods. (d) Same as panel (a), except that the trend was derived by using original (including gaps) satellite Chl data. Green and blue boxes in (b) are the subarctic and subtropical regions, respectively, where the time series of mean Chl anomaly data in Fig. 5 were derived.

**Fig. 5** (a) Time series of mean Chl anomaly (red bars) derived from the subarctic region (160–170ºE and 47–52ºN; see the green box in Fig. 4b) and the PDO index (black bars) within the period from September 1997 to June 2013. The solid red and black lines are regression lines for Chl and the PDO index, respectively. The dashed red and black lines are the same as the solid lines, except that the regression lines were derived from November 1997 to September 2007 (indicated by the vertical dashed blue line). Panel (b) is the same as panel (a) except that the mean Chl anomaly was derived from the subtropical region (130–140ºE and 24–30ºN; see the blue box in Fig. 4b).

**Table 1** Summary of Chl trends observed within the 16-year time span (September 1997 to June 2013) in different areas of interest and the probable responsible factors and/or mechanisms during each of the four seasons

| Season | Area of interest | Trend of Chl | Trend of environmental variables and probable factors/mechanisms |
|---|---|---|---|
| Winter | North of 42°N | Increase | Increased SST promoted phytoplankton growth<br>Increased MLD reduced grazing pressure |
| | South of 30°N | Decrease | Decreased MLD decreased nutrient availability |
| Spring | North of 46°N | Increase | Increased SST promoted phytoplankton growth |
| | Latitudes 36–46°N, east of 160°E | Decrease | Increased SST (by strengthening stratification) decreased nutrient availability;<br>Decreased PAR reduced light availability |
| | Oyashio area | Decrease | Increased MLD lengthened low-light period;<br>Decreased PAR reduced light availability;<br>Decreased SST decreased phytoplankton growth |
| | Along latitude 30°N | Weak increase | Increased MLD increased nutrient availability |
| Summer | North of 45°N | Increase | Increased SST promoted phytoplankton growth |
| | Oyashio area | Decrease | Decreased MLD decreased nutrient availability;<br>Decreased PAR decrease light availability;<br>Decreased MLD increased grazing pressure |
| | Along latitude 36°N | Weak increase | Unclear mechanisms |
| Fall | North of 45°N | Increase | Increased SST promoted phytoplankton growth;<br>Increased PAR increased light availability |
| | Oyashio area and along 42–45°N | Decrease | Decreased PAR reduced light availability;<br>Decreased MLD increased grazing pressure |
| | Latitudes 33–42°N, east of 160°E | Decrease | Increased SST (shoaled mixed layer) decreased nutrient supply |
| | South of Japan | Decrease | Decreased MLD decreased nutrient availability |
| | South of 30°N | Weak decrease | Increased SST (by strengthening stratification) decreased nutrient availability |

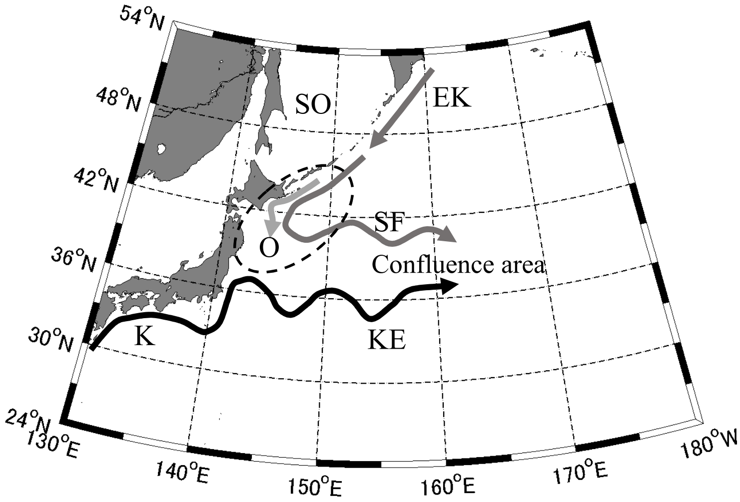
54°N
48°N
42°N
36°N
30°N
24°N
130°E
140°E
150°E
160°E
170°E
180°W
SO
EK
SF
O
Confluence area
K
KE

**Fig.** 1

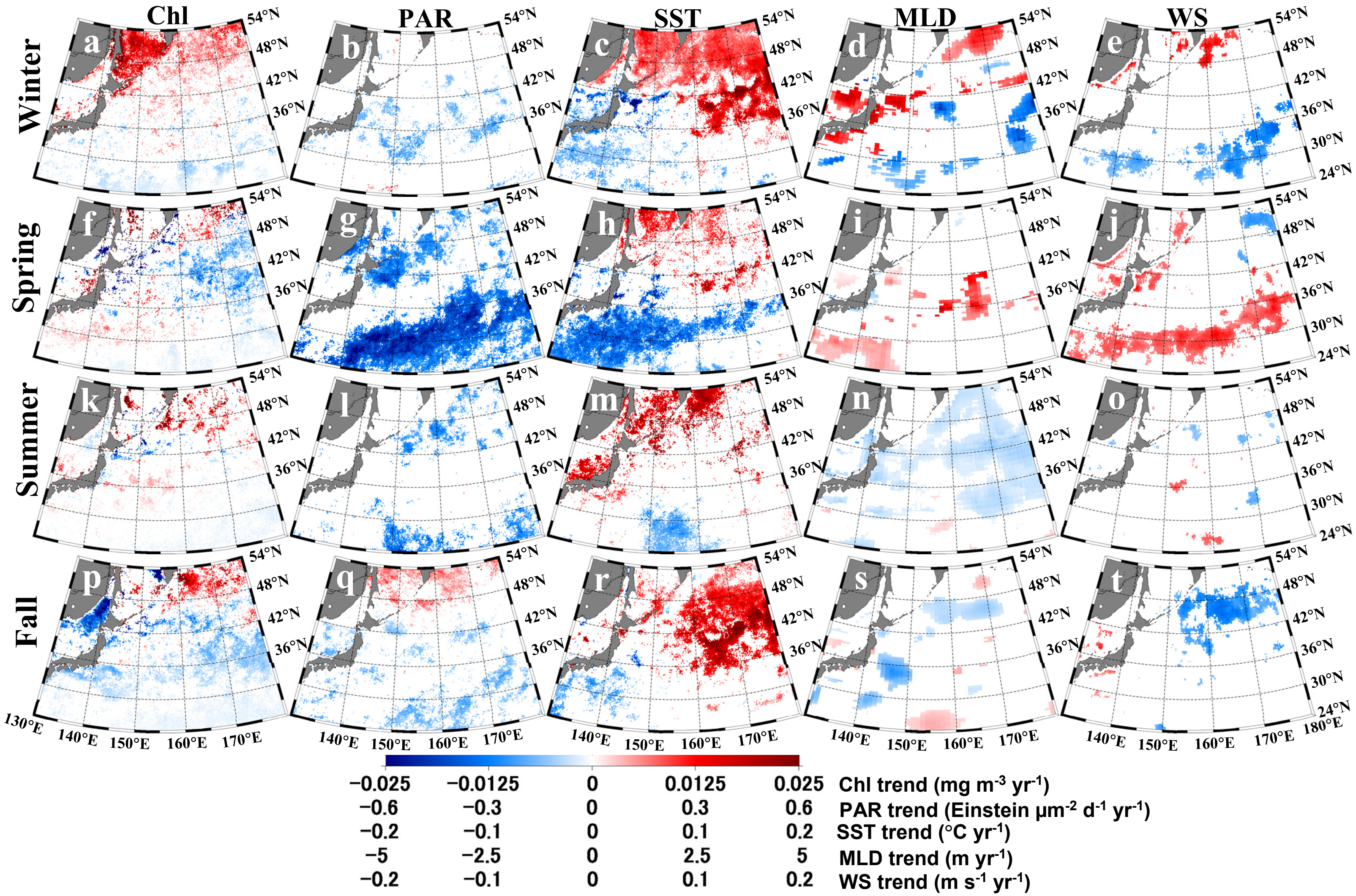
Chl
PAR
SST
MLD
WS
Winter
Spring
Summer
Fall
a
b
c
d
e
f
g
h
i
j
k
l
m
n
o
p
q
r
s
t
54°N
48°N
42°N
36°N
30°N
24°N
130°E
140°E
150°E
160°E
170°E
180°E
−0.025 −0.0125 0 0.0125 0.025 Chl trend (mg m-3 yr-1)
−0.6 −0.3 0 0.3 0.6 PAR trend (Einstein μm-2 d-1 yr-1)
−0.2 −0.1 0 0.1 0.2 SST trend (°C yr-1)
−5 −2.5 0 2.5 5 MLD trend (m yr-1)
−0.2 −0.1 0 0.1 0.2 WS trend (m s-1 yr-1)

**Fig.** 2

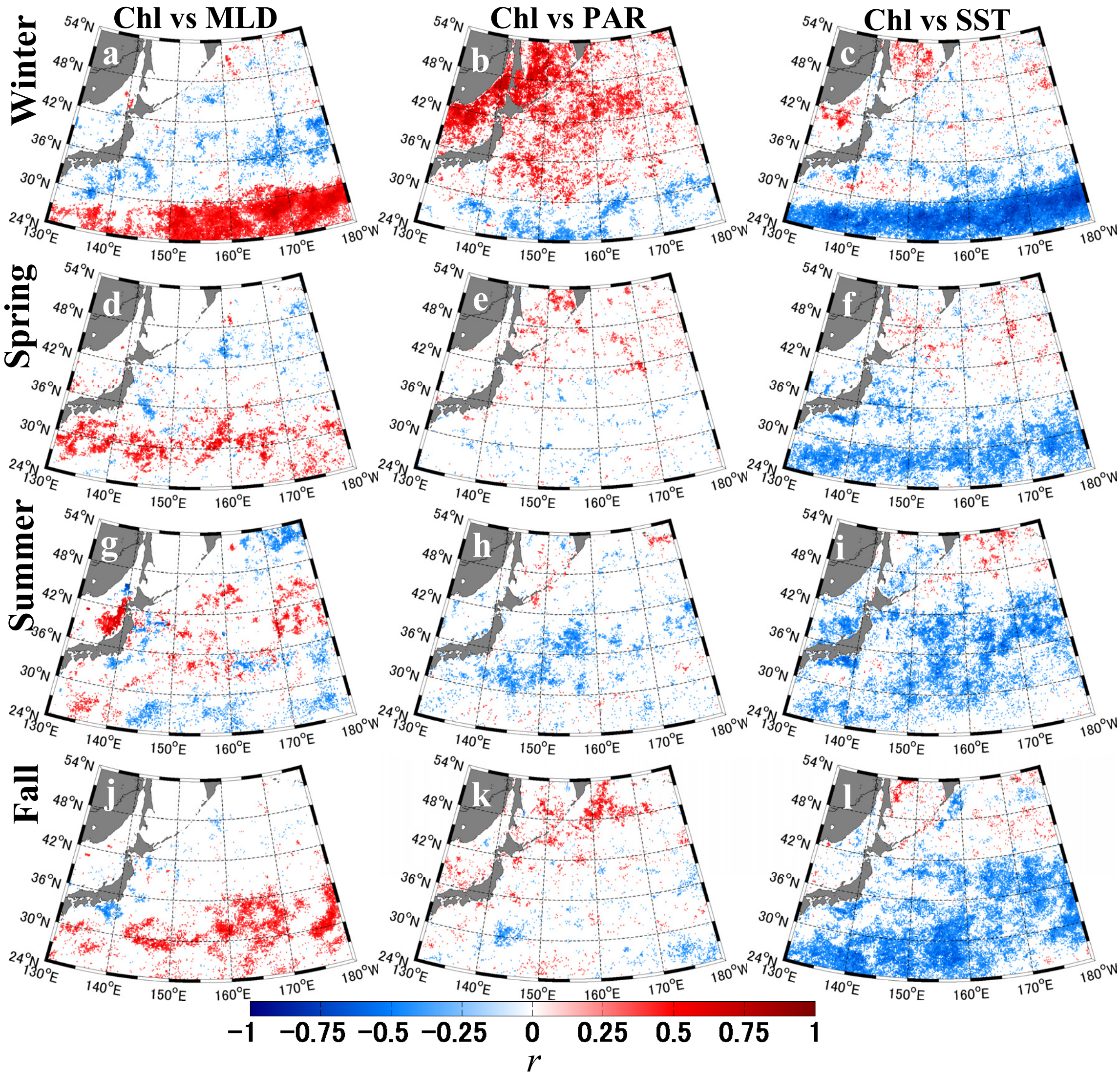
Chl vs MLD
Chl vs PAR
Chl vs SST
Winter
Spring
Summer
Fall
a
b
c
d
e
f
g
h
i
j
k
l
54°N
48°N
42°N
36°N
30°N
24°N
130°E
140°E
150°E
160°E
170°E
180°W
−1
−0.75
−0.5
−0.25
0
0.25
0.5
0.75
1
r

**Fig**. 3

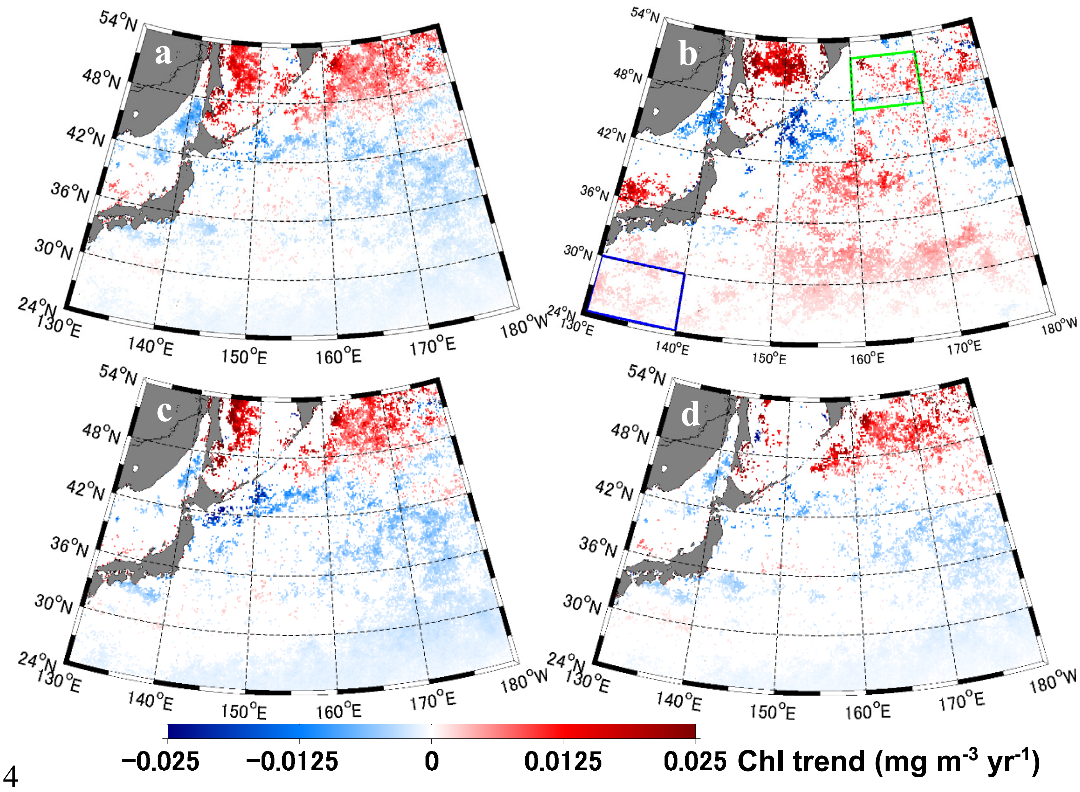

a
b
c
d
54°N
48°N
42°N
36°N
30°N
24°N
130°E
140°E
150°E
160°E
170°E
180°W
−0.025
−0.0125
0
0.0125
0.025
Chl trend (mg m-3 yr-1)


**Fig.** 4

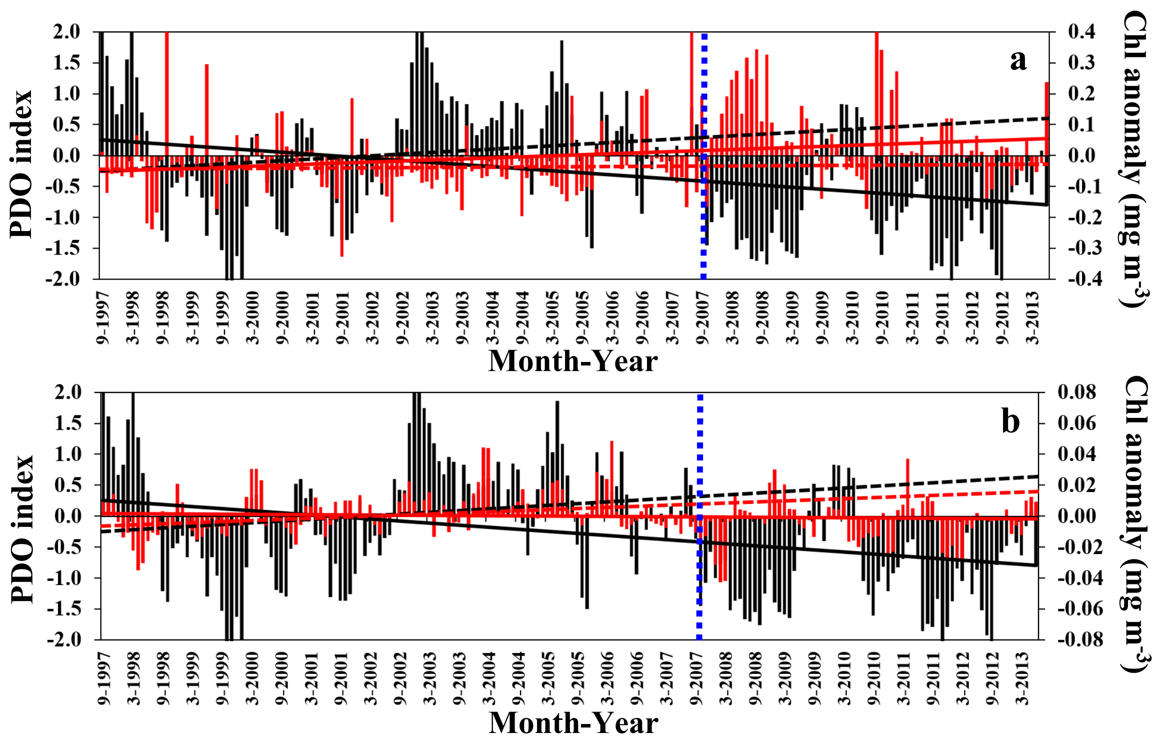

a
b
PDO index
Chl anomaly (mg m-3)
Month-Year


**Fig.** 5